

M. Egelhaaf · N. Böddeker · R. Kern · J. Kretzberg  
J. P. Lindemann · A.-K. Warzecha

## Visually guided orientation in flies: case studies in computational neuroethology

Received: 7 January 2003 / Revised: 10 April 2003 / Accepted: 11 April 2003 / Published online: 15 May 2003

**Abstract** To understand the functioning of nervous systems and, in particular, how they control behaviour we must bridge many levels of complexity from molecules, cells and synapses to perception behaviour. Although experimental analysis is a precondition for understanding by nervous systems, it is in no way sufficient. The understanding is aided at all levels of complexity by modelling. Modelling proved to be an inevitable tool to test the experimentally established hypotheses. In this review it will be exemplified by three case studies that the appropriate level of modelling needs to be adjusted to the particular computational problems that are to be solved. (1) Specific features of the highly virtuosic pursuit behaviour of male flies can be understood on the basis of a phenomenological model that relates the visual input to the motor output. (2) The processing of retinal image motion as is experienced by freely moving animals can be understood on the basis of a model consisting of algorithmic components and components which represent a simple equivalent circuit of nerve cells. (3) Behaviourally relevant features of the reliability of encoding of visual motion information can be understood by modelling the transformation of postsynaptic potentials into sequences of spike trains.

neurons, each of which has already highly complex functional properties. With their neuronal machinery even relatively small animals are able to do extraordinary things—at least if judged by comparison with man-made artificial systems. Think, for instance, of a hoverfly hovering in front of an object, suddenly sweeping to the side at a high velocity but returning within seconds to the same spot, or of the acrobatic flight manoeuvres of a male blowfly while pursuing another fly in the context of mating behaviour. During such astonishing manoeuvres information about the environment has to be gathered by the sense organs, processed rapidly by the nervous system, adjusted according to internally stored information, transformed into motor commands and eventually used to guide behaviour.

To understand the functioning of nervous systems and, in particular, how they control behaviour we must bridge many levels of analysis from molecules, cells and synapses to perception and behaviour. Although experimental analysis is a precondition for understanding information processing by nervous systems, it is in no way sufficient. In the 18th century the Italian philosopher Giambattista Vico proposed the principle that we can only understand what we make. Translating this principle to the study of brain function it means that in order to understand the brain we must ‘construct’ one and simulate the behaviour of the organism. Modelling brain function always entails the problem of the level of organisation at which the relevant features of the system can be grasped most appropriately. For instance, trying to model the behavioural performance of an entire animal on the basis of all molecules making up the involved nerve cells would be not only impossible but also an absurd encounter. Instead, a more promising approach is to model, and in this way to try to understand, the functioning of nervous systems via a series of progressively reductive levels of explanation. These levels range from a phenomenological characterisation of the performance of the entire system to a description of the biophysical properties of nerve cells and their synaptic

---

### Introduction

Brains are believed to belong to the most complex structures in the universe. They consist of densely packed and intricately interconnected networks of

---

M. Egelhaaf (✉) · N. Böddeker · R. Kern · J. Kretzberg  
J. P. Lindemann · A.-K. Warzecha  
Lehrstuhl für Neurobiologie, Fakultät für Biologie,  
Universität Bielefeld, Postfach 10 01 31,  
33501 Bielefeld, Germany  
E-mail: martin.egelhaaf@uni-bielefeld.de  
Tel.: +49-521-1065570  
Fax: +49-521-1066038

interactions, and even to an analysis of the subcellular computational mechanisms.

Visually guided orientation behaviour of flies has turned out to be one of the few cases in which it has been feasible to reach an understanding of mechanisms underlying complex behavioural performance at different levels of organisation (reviews: Reichardt and Poggio 1976; Hausen and Egelhaaf 1989, Egelhaaf and Borst 1993a, Egelhaaf and Warzecha 1999, Egelhaaf et al. 2002, Borst and Haag 2002, Egelhaaf and Kern 2002). The present review focuses on three examples of information processing that are currently being analysed and understood at widely divergent levels. Each of these examples pertains to the processing of behaviourally relevant visual information and addresses problems that are relevant far beyond the system that forms the basis for the experimental and model analysis.

### Pursuit behaviour: phenomenological modelling of virtuosic flight control

Male flies are able to chase females in often highly acrobatic visually guided flight manoeuvres. In up to ten saccadic turns per second with angular velocities of up to  $5000^\circ \text{ s}^{-1}$ , flies try to fixate the target fly in the frontal part of their visual field and to catch it as a first step in mating behaviour (Land and Collett 1974; Wagner 1986). In recent studies the control system underlying chasing behaviour could be largely unravelled at a phenomenological level. This has been possible mainly because a system analysis has been performed not only with real flies as targets but by using black spheres as dummy flies (Boeddeker et al. 2003). By this approach it has been possible to control to a large extent the visual input of the pursuing fly, even under free-flight conditions. Depending on the size and the velocity of the target, it is either caught after relatively short pursuit flights or it may be followed by the chasing fly for up to several seconds on precisely controlled tracks even if the target is not caught (Fig. 1A, upper diagram). The larger and the faster the dummy is, the less frequently it is caught (Fig. 1C, upper diagram). During such 'unsuccessful' chases, larger and faster dummies are followed at larger distances than are small and relatively slow ones. As a consequence of this strategy, the retinal size of the target is kept approximately constant for a given target velocity irrespective of the absolute target size. However, the retinal size decreases with increasing velocity of the target (Fig. 1D, upper diagram).

Model simulations employing a two-dimensional phenomenological model of the fly's control system for chasing revealed that both modes of chasing behaviour (catching of the target and tracking without catching it) can be mediated by a single control system without requiring any explicit 'decision-maker' (N. Boeddeker and M. Egelhaaf, unpublished observations). The different behavioural modes of the model fly are a consequence of the peculiar properties of two visual

**Fig. 1A–D** Chasing behaviour of freely flying flies and of their model equivalents. **A** Flight trajectories of a real (*upper panels*) and model fly (*bottom panels, grey background*) chasing a spherical target moving on a circular path (radius: 100 mm). *Left*: flight trajectory of a fly capturing the target. *Right*: pursuit of the target without capture. The trajectories of the real fly are reconstructed from videotaped behavioural experiments. The fly is indicated by the position of its centroid (*circle*) and the orientation of the body axis (*line*). The *numbers* denote corresponding positions of the fly and the target in intervals of 100 ms. *Calibration bars*: 50 mm. **B** Model of the chasing system. The model fly consists of two parallel pathways, one for speed control (*left*) and one for target fixation (*right*). The outputs of both controllers are fed into first-order low-pass temporal filters which differ in their time constants (see *insets* for step responses of the filters). These temporal filters mimic neuronal processing and muscular reaction time. The weighted outputs of each pathway form the 'intended' vector (*black solid line*) of locomotion of the model fly, as is represented at its motor output. In the next processing step of the model the kinematics of fly body movements is emulated by forward Euler integration: The weighted intended vector and the weighted actual velocity vector of the model fly summated (*dashed black line*). The outcome of this summation determines the model fly's position in the next simulation step (*grey fly icon*). The actual velocity of the model fly in the next simulation step (*grey solid line*) is different from the intended vector of locomotion the step before which in real flight manoeuvres would be caused by friction and inertia. Data is updated 1,000 times per simulated second. **C** Dependence of the probability of target capture on target size and target speed in behavioural experiments (*upper panel*). The percentage gives the portion of captures among all chases for a given combination of target parameters. *Lower panel*: the percentage of captures in model simulations when the starting position and orientation of the model fly is varied in the simulated arena. **D** Dependence of retinal target size on the absolute size and the velocity of the target. *Upper panel*: box-and-whisker plots of the maximal retinal size (visual angle) of the target in each chase without target capture in behavioural experiments. The box has horizontal lines at the lower quartile, median, and upper quartile values. The lines extending from each end of the box show the extent of the rest of the data. The retinal size was calculated as the median of all local maxima of the time dependent retinal size for each chase. *Left*: differently sized targets at a speed of  $1.5 \text{ m s}^{-1}$ . *Right*: pursuits after the 13-mm-sized target at the three different speeds. *Lower panel*: in the model simulations the retinal size achieves, after an initial transient response, a steady state if the target is not captured. The steady-state retinal size for different sized targets (*large markers*: 13 mm, *small markers*: 8.3 mm) is shown for different target velocities. Note the different scaling compared to the upper panel in **D** (for details see Boeddeker et al. 2003)

mechanisms working partly in parallel. These two mechanisms control the forward and angular velocity of the simulated animal, respectively. Whereas the retinal size of the target controls the forward velocity of the chasing male, the retinal position of the target determines the fly's flight direction. Low-pass filters in either branch of the model representing the two mechanisms simulate neuronal processing time. The kinematics of a fly's movements is emulated by the computationally cheap forward Euler integration (see Fig. 1B for an explanation).

The model fly shows similar behaviour as real flies. Depending on the size and the velocity of the target as well as on the starting position and orientation of the chasing fly, the target is either caught or followed in a similar way as observed in the behavioural experiments

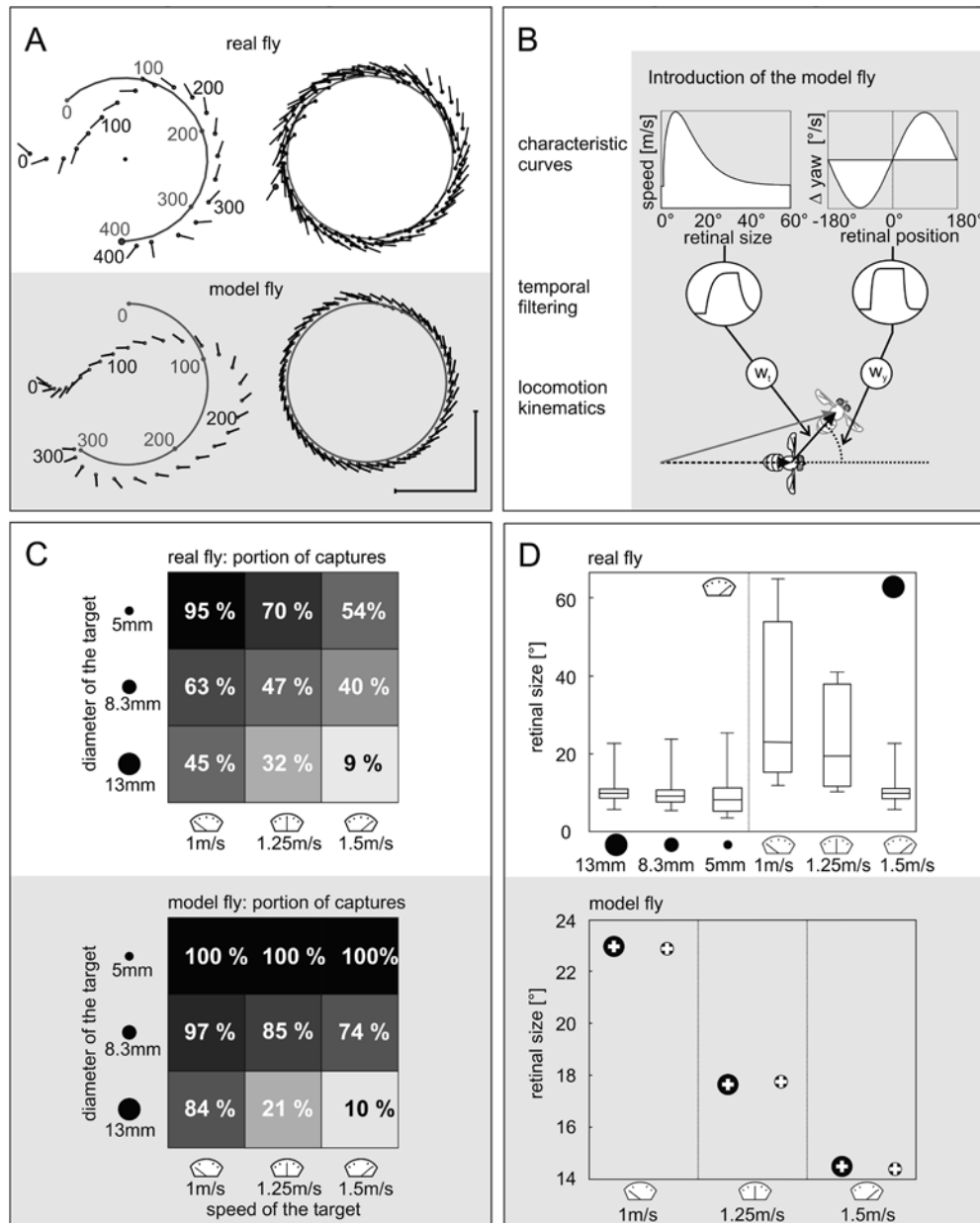


(Fig. 1A). Large targets are caught only if the model fly reaches a high velocity during the approach. During chases without success the model fly keeps, in a similar way as real flies, the target at a constant retinal size for a given target speed. Increasing the speed of the target results in a smaller retinal size as is the case in the behavioural experiments (Fig. 1D). Prior to successful approaches the chasing fly flies at a higher forward velocity than the target. The chasing fly decelerates when, during an approach, the retinal size of the target exceeds a critical value. Despite the deceleration, targets of appropriate size and velocity are caught with high probability. The larger the target the larger is the distance at which the chasing fly starts to decelerate, because the critical retinal size is reached earlier. This is the reason for the lower catch frequencies of large targets

(Fig. 1C). The distance between the chasing fly and a large target is overcome only if the speed difference is very high and the higher momentum of the chasing fly is sufficient to overcome the spatial gap between pursuer and target (Boeddeker et al. 2003; N. Boeddeker and M. Egelhaaf, unpublished observations).

The phenomenological model of the chasing control system is not only sufficient to account for pursuits of artificial targets but also of real flies flying on much more complicated courses. Although only a smooth pursuit system has been implemented in the model and the chasing fly translates the retinal position of the target into angular velocity in a continuous way, the model fly shows body 'saccades' with rapid changes of body axis orientation. These saccades can be explained as the consequence of inertia and the different time constants

of the low-pass filters in the pathways controlling the angular and the forward velocity, respectively (N. Boeddeker and M. Egelhaaf, unpublished observations). Although chasing after real flies can be explained by the simple model sketched in Fig. 1B, pursuit behaviour is stabilised if the system controlling angular velocity not only depends on the retinal position of the target, but also its velocity (Land 1992; N. Boeddeker and M. Egelhaaf, unpublished observations).

Flies are concluded to employ similar viewing strategies as primates: spontaneous changes in gaze are done rapidly in a saccadic manner (Hateren and Schilstra 1999; Schilstra and Hateren 1998, 1999), whereas moving targets are followed by smooth pursuit (Boeddeker et al. 2003). Nonetheless, the angular velocities flies may reach during smooth pursuit are much higher than eye velocities of humans (Ilg 1997).

### Processing of natural retinal image sequences: transfer of models established by systems analysis with simple visual input to naturalistic conditions

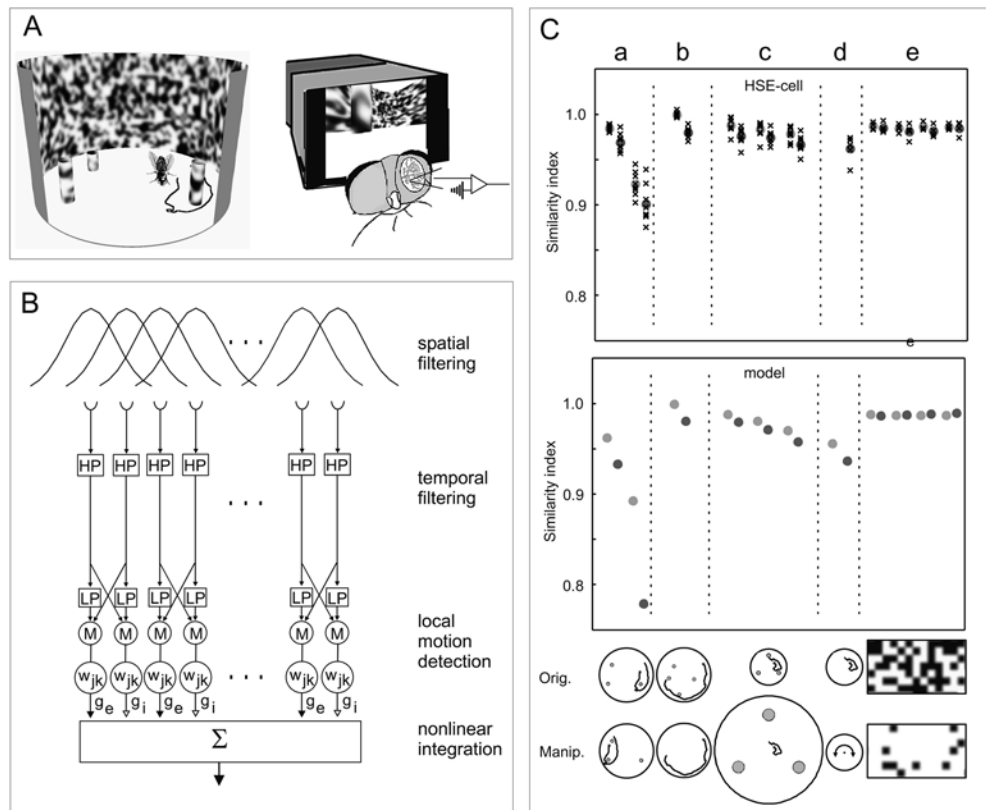
Phenomenological models, such as the model of pursuit control, provide information about the visual parameters that are relevant for controlling a particular behavioural component. However, they do not account for the computations extracting the relevant visual information from the retinal images. In the context of optomotor course control it has been possible during recent years to elucidate relevant computations in terms of formal computational models and, partly, even in terms of the biophysical properties of individual nerve cells and their synaptic interactions (reviews: Egelhaaf et al. 2002; Borst and Haag 2002).

Optomotor course control relies to a large extent on neuronal analysis of the continual displacements of the retinal images of the entire environment, as is characteristic of self-motion. It is known that this so-called optic flow is evaluated by the visual systems of many animals and used to control the animals' path of locomotion. In the fly optic flow processing has been analysed in unprecedented detail at the neuronal level and much is known about the underlying neuronal circuits (reviews: Hausen and Egelhaaf 1989; Egelhaaf and Borst 1993a; Egelhaaf and Warzecha 1999, Krapp 2000; Borst and Haag 2002; Egelhaaf et al. 2002; Egelhaaf and Kern 2002). These circuits have been mainly established in systems analyses using relatively simple stimuli, and part of the underlying computations could be successfully modelled both algorithmically and on the basis of electrical equivalent circuits that are employed to approximate individual neurons. Recently, thanks to advances in computer technology, the performance of the neuronal circuits could be analysed with the complex visual inputs that are characteristic of natural behavioural situations.

The dynamics of optic flow are largely determined by the dynamics of the animal's self-motion. The direction

**Fig. 2A–C** Responses of a motion sensitive neuron and its model equivalent to naturalistic optic flow as experienced by a walking fly. **A** Experimental approach. Flies walking freely in an arena are video recorded (*left*). The video is grabbed off-line frame by frame and the position and orientation of the fly is determined in each digitised video frame. The trajectory data are used to control the path of a simulated camera in a virtual 3-D environment that mimics the arena. The size of the field of view of the camera is adjusted to match the receptive field properties of the cell to be recorded from in subsequent electrophysiological experiments. In the electrophysiological experiments the motion sensitive neuron is visually stimulated by the sequence of reconstructed images (*right*). **B** Schematic of the model of the fly's motion pathway. For the sake of clarity only one horizontal dimension of the model is sketched. The input layer of the model consists of a matrix of  $62 \times 62$  retinotopically organised elements. There are three major processing stages (peripheral prefiltering, local motion detection, nonlinear integration of local motion signals). *HP* temporal first-order high-pass filter; *LP* temporal first-order low-pass filter; *M* multiplication stage of the elementary movement detector;  $w_{jk}$  constant weight factors which adjust the spatial sensitivity distribution of the output cell of the model to that of the real cell;  $g_e$ ,  $g_i$  gain factors of the excitatory and inhibitory output channels of the elementary movement detectors, controlling excitatory and inhibitory conductances;  $\Sigma$  nonlinear integration of the local motion signals. **C** Similarity of responses of the HSE-cell (*upper diagram*) and its model equivalent (*bottom diagram*) to various original optic flow stimuli and to manipulated versions of them. The similarity index is given by the ratio of the peak of the normalised cross-correlation of individual responses of the original and manipulated stimuli to the peak of the normalised cross-correlation of individual responses to the original stimulus. A similarity index of 1 means for the experimental results that the time-courses of individual responses obtained under the two different stimulus conditions are as similar as the time-courses of individual responses obtained under the same stimulus condition (*crosses*: results for individual cells; *filled circles*: mean results). For each pair of original and manipulated stimulus conditions, the left data points refer to the responses of the left HSE cell or its model equivalent, the right data points refer to the right cells. Part of the manipulations are illustrated in the *insets*. *Filled circles within insets* denote the position and diameter of objects in the arena. Stimulus situations from left to right: *a* Similarity of responses to the track in its original position versus the track displaced to the centre of the arena (*left*), and the track in its original position versus the track displaced to the opposite side of the arena (*right*); *b* Three objects present during the original walk of the fly were removed; *c* The arena was enlarged by a factor of 1.5, 2.0 and 3.0 (data from left to right). The enlargement includes the objects as well as the pattern on the arena wall and on the objects; the position of the track with respect to the arena centre was kept the same; *d* The translational component of the original walking track was eliminated and the fly rotated around the arena centre. No objects were present in the arena; *e* The original 50% black and white texture was exchanged by a texture with only 12% black elements. This was done and tested for the originally sized arena as well as for the arena enlarged by a factor of 1.5, 2.0, and 3.0 (data shown from left to right). The texture density of the patterns covering the objects were kept as in the originally sized arena. The enlargement of the arena includes the pattern on the arena wall and on the objects (for details see (Kern et al. 2001b)

of self-motion may change rapidly, as during saccadic turns during flight (Schilstra and Hateren 1999; Hateren and Schilstra 1999) or, one order of magnitude more slowly, during walking (Kern et al. 2001a). Because it is currently not possible to record from neurons in freely moving flies, the optic flow experienced by behaving flies was reconstructed and replayed to tethered animals during nerve cell recordings. This approach has been



employed for various behavioural situations during tethered flight in a flight simulator (Warzecha and Egelhaaf 1997; Kimmerle and Egelhaaf 2000), during unrestrained walking in a three-dimensional environment (Kern et al. 2000, 2001a) (Fig. 2A) and most recently during unrestrained flight (Lindemann et al. 2003).

These analyses suggest that information obtained from optic flow about the animal's self-motion during walking (Kern et al. 2001a) is much less ambiguous than was concluded from previous studies using conventional stimuli. For instance, an identified motion-sensitive neuron whose input connections suggest a role in signalling turns of the animal around its vertical axis (Hausen 1981; Horstmann et al. 2000; Haag and Borst 2001) also responds to translation and to changes in the texture of conventional stimuli (Hausen 1981; Hausen and Egelhaaf 1989; Kern et al. 2001a). However, when challenged with optic flow as experienced during walking, most of the ambiguities do not emerge and the cell provides information about the animal's turning direction largely independent of the translational optic flow component and the layout of the environment (Kern et al. 2001a) (Fig. 2C, upper diagram). Only when the animal comes very close to an object are the neuronal responses considerably affected by the environmental features and thus may provide information about the three-dimensional layout of the environment.

Model simulations indicate that the computations underlying optic flow processing are well matched to

optic flow experienced in behavioural situations (Kern et al. 2001b). The model used is an elaboration of models previously established to explain various aspects of motion detection by the fly visual system if characterised with simple stimuli. It is a hybrid of algorithmic components and components which represent a simple equivalent circuit of a nerve cell (Fig. 2B). Spatio-temporal filters model the peripheral part of the motion detection pathway, i.e. the retina and the first visual neuropile. The resulting signals are fed into correlation-type motion detectors, which have been shown to explain many aspects of the local motion detector (EMD) responses in the fly's visual system (review: Egelhaaf and Borst 1993b). Although the output of this part of the model is meant to fit the output of the local motion detectors of the fly, it is not intended to approximate the cellular operations in detail. A simple equivalent circuit of a patch of passive membrane achieves spatial pooling of many local motion detectors. Excitatory and inhibitory conductances of this membrane are controlled by the positive and negative outputs of the local motion detectors, respectively (Borst et al. 1995; Single et al. 1997). The model output can be interpreted as representing the time-dependent graded postsynaptic potential of the above-mentioned motion-sensitive neuron.

On the basis of this network model not only many relevant response features of fly motion sensitive neurons discovered with conventional stimuli can be explained, but also those discovered with complex naturalistic optic flow. In particular, the model output is

robust against a wide range of manipulations of the visual input of walking flies in a similar way as the responses of fly motion-sensitive neurons (Kern et al. 2001b). For instance, very similar responses are obtained in both the real and the model cell to the optic flow experienced on tracks, corresponding to the original walking track after displacing it to other sites in the experimental arena. Moreover, eliminating the translational component from the optic flow does not much alter the responses (Fig. 2C, compare upper and lower panels). Hence, naturalistic optic flow experienced by walking flies, is represented by the model output, in accordance with the neuronal data, less ambiguously than conventional stimuli, as long as the animal is not too close to objects in its environment (Kern et al. 2001b). A recent model analysis (J.P. Lindemann et al., unpublished observations) indicates that this is because (1) natural stimuli are characterised by a wide range of spatial frequencies (in contrast to conventional grating patterns (see also Dror et al. 2001), (2) the rotational optic flow component dominates the translational one apart from situations when the animal is close to objects, (3) the motion input of motion-sensitive neurons exceeds the dynamic range where the time-course of velocity is represented linearly (Egelhaaf and Reichardt 1987), and (4) the non-linear spatial integration characteristics of the motion-sensitive neurons make their responses largely independent of texture density (Borst et al. 1995; Single et al. 1997).

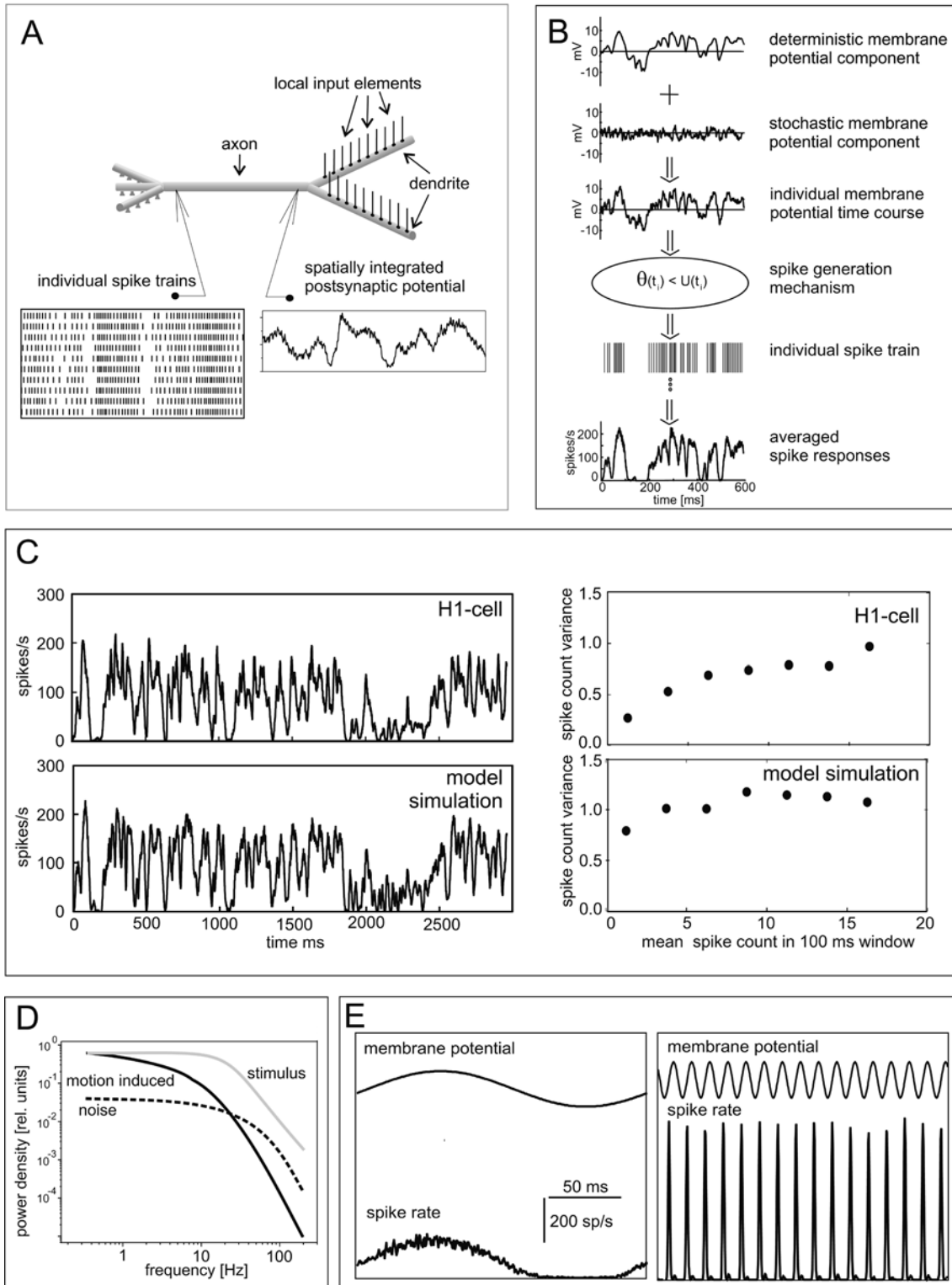
### **Precision of neuronal encoding of visual motion information: modelling the transformation of postsynaptic potentials into spike trains**

The models of visual information processing described above can explain major aspects of the time-dependent performance of the fly or particular neuronal subsystems even under complex dynamical conditions as occur in behavioural situations. In these models the output of the visual system is given by analogue signals that encode some features of the retinal input in a graded way. However, these do not take into account that graded postsynaptic potentials in nerve cells are often transformed into spike trains and that neuronal responses are not entirely deterministic, but show much variability (Fig. 3A). The spike count variance across trials of fly motion-sensitive neurons is relatively small compared to motion-sensitive neurons in the primate cortex (Warzecha and Egelhaaf 1999; Warzecha et al. 2000; Barberini et al. 2000). Nevertheless, the precision with which stimulus events can be encoded by the timing of spikes and, thus, the accuracy with which time-varying optic flow characteristic of behavioural situations can be conveyed are constrained by the variability of neuronal responses.

The transformation of graded postsynaptic signals into spike trains has recently been modelled in detail for motion sensitive neurons of the fly. Compartmental

**Fig. 3A–E** Variability of neuronal responses and timescale on which visual motion information is signalled. **A** Schematic illustrating the transformation of summated postsynaptic membrane potential fluctuations into spike trains. The neuron receives synaptic input from many local motion-sensitive elements. The postsynaptic potentials are summated and transformed into spike trains that reach the output region of the cell. Subsequent sample traces of individual responses to repetitive presentations of the same motion trace plotted underneath each other. Each *vertical line* denotes the occurrence of a spike. Although the overall pattern of the neuronal activity is similar from trial to trial, there is variability in the temporal fine structure across trials. **B** Sketch of a phenomenological model of spike generation. The spike generation mechanism is fed by summated postsynaptic potential fluctuations. These consist of a deterministic membrane potential component that is the same for each presentation of a given visual motion stimulus and membrane potential noise that differs for each stimulus presentation. The individual spike trains can be averaged to obtain a spike frequency histogram (for details see Kretzberg et al. 2001). **C** Spike frequency histogram of a motion-sensitive H1 cell and of the corresponding model cell (*left panels*). Random velocity fluctuations were used for motion stimulation leading to wildly varying modulations in spike frequency. The variance of the spike count in 100-ms time windows depends in a similar way in both the H1 cell and the model cell on the mean spike count (*right panels*) (for details see Warzecha et al. 2000; Kretzberg et al. 2001). **D** Schematic of the dynamical properties of membrane potential fluctuations of a fly motion-sensitive neuron elicited by band-limited white-noise velocity fluctuations. Power spectra of the motion stimulus, the motion-induced response component and the membrane potential noise. The motion-induced response component is determined by averaging many individual response traces and thereby eliminating the membrane potential noise. The motion-induced response has most of its power below 20 Hz although the stimulus contained higher frequencies. In the low-frequency range the motion-induced response component is larger than the noise component. Towards higher frequencies this relationship reverses. Spikes time-lock to the fast stochastic membrane potential fluctuations (for details see Warzecha et al. 1998). **E** Time-locking of spikes to sinusoidal membrane potential fluctuations in a model cell. The model is adjusted to fit the responses of a fly neuron to motion stimuli. The deterministic component of the membrane potential, as may be induced by a stimulus, fluctuates sinusoidally with either 5 Hz (*upper trace, left panel*) or 80 Hz (*upper trace, right panel*). To simulate the responses to repetitive presentations of the same stimulus, the deterministic component is superimposed by membrane potential noise that differs from presentation to presentation. Spike frequency histograms (*bottom traces*) illustrate that fast membrane potential fluctuations are needed to trigger spikes with a high temporal precision. Slow fluctuations lead to spike activity with a rate about proportional to the membrane potential (for details see (Kretzberg et al. 2001)

models of fly motion-sensitive neurons have been developed that take into account both the complex geometrical structure as well as the intricate biophysical properties of the neurons. These models include the passive membrane properties as well as ionic currents modelled on the basis of Hodgkin-Huxley equations, as they could be characterised experimentally (Borst and Haag 1996; Haag et al. 1997, 1999; Haag and Borst 2000). These models reproduce many features of the experimental data on which they are based and may also account for the characteristic variability of the neuronal responses. However, for a systematic analysis of this important aspect of neuronal coding simpler



phenomenological models of spike generation proved to be sufficient to account for a wide range of computationally relevant phenomena.

The precision of spike responses to sensory stimuli depends on the dynamics of the postsynaptic membrane potential fluctuations induced by the stimulus and those

that are not related to the stimulus, i.e. membrane potential noise. This conclusion is based on a combination of model simulations and dual recordings from pairs of motion sensitive neurons that share large parts of their synaptic input (Warzecha et al. 1998). The model analysis was based on a phenomenological model of spike

generation that transforms membrane potential traces into spike trains (Fig. 3B). In the model the timing of spikes depends on the time elapsed since the previous action potential and on the preceding membrane potential changes. Fed with a combination of stimulus-induced membrane potential fluctuations and membrane potential noise, as they were determined experimentally, the model reproduces the time-course and variability of neuronal spike responses well (Fig. 3C). Fast stimulus-induced membrane potential fluctuations are needed to trigger spikes with a high temporal precision in the presence of membrane potential noise. Slow fluctuations lead to spike activity with a rate about proportional to the membrane potential (Warzecha et al. 2000; Kretzberg et al. 2001). Thus, for a given level of membrane potential noise the frequency range of membrane potential fluctuations induced by a stimulus determines whether a neuron can use a rate code or a temporal code. Since the computations underlying motion detection inevitably require time constants of some tens of milliseconds (Borst and Egelhaaf 1989), they attenuate the neural responses to high-frequency fluctuations in pattern velocity (Haag and Borst 1997; Warzecha et al. 1998, 2003) (Fig. 3D). Hence, only when the velocity changes are very rapid and large the resulting depolarisations of the motion-sensitive neuron are sufficiently pronounced to elicit spikes with a millisecond precision (Ruyter van Steveninck and Bialek 1995; Warzecha and Egelhaaf 2001; Ruyter van Steveninck et al. 2001; Warzecha et al. 2003). Otherwise, the exact timing of spikes is determined mostly by membrane potential noise and visual motion is most likely represented by the spike rate (Fig. 3E) (Kretzberg et al. 2001).

## Conclusions

It is now possible to understand visual information processing in the fly visual system at various levels of complexity, ranging from free-flight behaviour down to the biophysical properties of individual nerve cells. The understanding is aided at all these levels by modelling. Modelling proved to be an essential tool to test the experimentally established hypotheses concerning the functioning of the system at the particular level of investigation. As is exemplified by the three case studies outlined here, the appropriate level of modelling needs to be adjusted to the particular computational problems that are to be solved. Of course, one major aim of our current analyses on visual information processing in the fly is to bridge the gap between different levels of analysis. In addition, neuronal models will substitute phenomenological and algorithmic models. For instance, the phenomenological model of the chasing system will be transformed into a cellular model in order to make predictions on the organisation of the underlying neuronal networks. However, to be able to proceed in this direction, we first need more experimental data on the

neuronal basis of chasing behaviour. A transformation of phenomenological into neuronal models is also desirable for the computations of visual motion detection in order to understand the underlying cellular mechanisms. In any case, the choice of a particular level of modelling should always be guided by scientific problems at the respective level of analysis.

Although we now understand important aspects of visual information processing, we are still far from being able to construct brains, even relatively simple ones such as that of the fly. Nonetheless, components of the current models have been implemented in hardware and tested in robots (Franceschini et al. 1992; Franceschini 1996; Bains 1999; Harrison and Koch 2000; Huber et al. 1999; Liu and Usseglio-Viretta 2000). All these robots still have a much simpler behavioural repertoire than real flies and, in particular, are by orders of magnitudes slower and much less virtuosic. Hence, still much needs to be learnt from real flies in future research, both experimentally and computationally, before we may be able to construct an artificial system which is able to perform similarly well as the real nervous system. Only then we may eventually understand by what computational principles the often astonishing behavioural performance is accomplished.

**Acknowledgements** We are grateful to J. Grewe, K. Karameier and R. Kurtz for critically reading a previous version of the paper. Our work is supported by the Deutsche Forschungsgemeinschaft (DFG).

## References

- Bains S (1999) A machine with a fly's-eye view. *Science* 285:1472
- Barberini CL, Horwitz GD, Newsome WT (2000) A comparison of spiking statistics in motion sensing neurons of flies and monkeys. In: Zanker JM, Zeil J (eds) *Computational, neural and ecological constraints of visual motion processing*. Springer, Berlin Heidelberg New York
- Boeddeker N, Kern R, Egelhaaf M (2003) Chasing a dummy target: smooth pursuit and velocity control in male blowflies. *Proc R Soc Lond Ser B* 270:393–399
- Borst A, Egelhaaf M (1989) Principles of visual motion detection. *Trends Neurosci* 12:297–306
- Borst A, Haag J (1996) The intrinsic electrophysiological characteristics of fly lobula plate tangential cells. I. Passive membrane properties. *J Comp Neurosci* 3:313–336
- Borst A, Haag J (2002) Neural networks in the cockpit of the fly. *J Comp Physiol A* 188:419–437
- Borst A, Egelhaaf M, Haag J (1995) Mechanisms of dendritic integration underlying gain control in fly motion-sensitive interneurons. *J Comput Neurosci* 2:5–18
- Dror RO, O'Carroll DC, Laughlin SB (2001) Accuracy of velocity estimation by Reichardt correlators. *J Opt Soc Am A* 18:241–252
- Egelhaaf M, Borst A (1993a) A look into the cockpit of the fly: visual orientation, algorithms, and identified neurons. *J Neurosci* 13:4563–4574
- Egelhaaf M, Borst A (1993b) Movement detection in arthropods. In: Wallman J, Miles FA (eds) *Visual motion and its role in the stabilization of gaze*. Elsevier, Amsterdam, pp 53–77
- Egelhaaf M, Kern R (2002) Vision in flying insects. *Curr Opin Neurobiol* 12:699–706

- Egelhaaf M, Reichardt W (1987) Dynamic response properties of movement detectors: theoretical analysis and electrophysiological investigation in the visual system of the fly. *Biol Cybern* 56:69–87
- Egelhaaf M, Warzecha A-K (1999) Encoding of motion in real time by the fly visual system. *Curr Opin Neurobiol* 9:454–460
- Egelhaaf M, Kern R, Krapp HG, Kretzberg J, Warzecha A-K (2002) Neural encoding of behaviourally relevant motion information in the fly. *Trends Neurosci* 94:94–100
- Franceschini N (1996) Engineering applications of small brains. *FED J* 7:38–52
- Franceschini N, Pichon JM, Blanes C (1992) From insect vision to robot vision. *Philos Trans R Soc Lond B* 337:283–294
- Haag J, Borst A (1997) Encoding of visual motion information and reliability in spiking and graded potential neurons. *J Neurosci* 17:4809–4819
- Haag J, Borst A (2000) Spatial distribution and characteristics of voltage-gated calcium signals within visual interneurons. *J Neurophysiol* 83:1039–1051
- Haag J, Borst A (2001) Recurrent network interactions underlying flow-field selectivity of visual interneurons. *J Neurosci* 21:5685–5692
- Haag J, Theunissen F, Borst A (1997) The intrinsic electrophysiological characteristics of fly lobula plate tangential cells. II. Active membrane properties. *J Comput Neurosci* 4:349–369
- Haag J, Vermeulen A, Borst A (1999) The intrinsic electrophysiological characteristics of fly lobula plate tangential cells. III. visual response properties. *J Comput Neurosci* 7:213–234
- Harrison RR, Koch C (2000) A silicon implementation of the fly's optomotor control system. *Neural Comput* 12:2291–2304
- Hateren JH von, Schilstra C (1999) Blowfly flight and optic flow. II. Head movements during flight. *J Exp Biol* 202:1491–1500
- Hausen K (1981) Monocular and binocular computation of motion in the lobula plate of the fly. *Verh Dtsch Zool Ges* 74:49–70
- Hausen K, Egelhaaf M (1989) Neural mechanisms of visual course control in insects. In: Stavenga D, Hardie RC (eds) *Facets of vision*. Springer, Berlin Heidelberg New York, pp 391–424
- Horstmann W, Egelhaaf M, Warzecha A-K (2000) Synaptic interactions increase optic flow specificity. *Eur J Neurosci* 12:2157–2165
- Huber SA, Franz MO, Bülthoff HH (1999) On robots and flies: modeling the visual orientation behavior of flies. *Robot Auton Syst* 29:227–242
- Ilg UJ (1997) Slow eye movement. *Progr Neurobiol* 53:293–329
- Kern R, Lutterklas M, Egelhaaf M (2000) Neural representation of optic flow experienced by unilaterally blinded flies on their mean walking trajectories. *J Comp Physiol A* 186:467–479
- Kern R, Peterleit C, Egelhaaf M (2001a) Neural processing of naturalistic optic flow. *J Neurosci* 21:1–5
- Kern R, Lutterklas M, Peterleit C, Lindemann JP, Egelhaaf M (2001b) Neuronal processing of behaviourally generated optic flow: experiments and model simulations. *Network Comput Neural Syst* 12:351–369
- Kimmerle B, Egelhaaf M (2000) Performance of fly visual interneurons during object fixation. *J Neurosci* 20:6256–6266
- Krapp HG (2000) Neuronal matched filters for optic flow processing in flying insects. In: Lappe M (ed) *Neuronal processing of optic flow*. Academic Press, San Diego, pp 93–120
- Kretzberg J, Egelhaaf M, Warzecha A-K (2001) Membrane potential fluctuations determine the precision of spike timing and synchronous activity: a model study. *J Comput Neurosci* 10:79–97
- Land MF (1992) Visual tracking and pursuit: Humans and arthropods compared. *J Insect Physiol* 38:939–951
- Land MF, Collett TS (1974) Chasing behaviour of houseflies (*Fannia canicularis*). A description and analysis. *J Comp Physiol* 89:331–357
- Lindemann JP, Kern R, Michaelis C, Meyer P, Hateren JH van, Egelhaaf M (2003) *FliMax*, a novel stimulus device for panoramic and highspeed presentation of behaviourally generated optic flow. *Vision Res* 43:779–791
- Liu S-C, Usseglio-Viretta A (2000) Visuo-motor fly-like responses of a robot using a VLSI motion-sensitive chip. *Proc 2nd ICSC Symp Neural Comput*
- Reichardt W, Poggio (1976) Visual control of orientation behaviour in the fly. Part I. A quantitative analysis. *Q Rev Biophys* 9:311–375
- Ruyter van Steveninck Rd, Bialek W (1995) Reliability and statistical efficiency of a blowfly movement-sensitive neuron. *Philos Trans R Soc Lond B* 348:321–340
- Ruyter van Steveninck Rd, Borst A, Bialek W (2001) Real-time encoding of motion: answerable questions and questionable answers from the fly's visual system. In: Zanker JM, Zeil J (eds) *Motion vision*. Springer, Berlin Heidelberg New York, pp 279–306
- Schilstra C, Hateren JH von (1998) Stabilizing gaze in flying blowflies. *Nature* 395:654
- Schilstra C, Hateren JH von (1999) Blowfly flight and optic flow. I. Thorax kinematics and flight dynamics. *J Exp Biol* 202:1481–1490
- Single S, Haag J, Borst A (1997) Dendritic computation of direction selectivity and gain control in visual interneurons. *J Neurosci* 17:6023–6030
- Wagner H (1986) Flight performance and visual control of the flight of the free-flying housefly (*Musca domestica*). II. Pursuit of targets. *Philos Trans R Soc Lond B* 312:553–579
- Warzecha A-K, Egelhaaf M (1997) How reliably does a neuron in the visual motion pathway of the fly encode behaviourally relevant information? *Eur J Neurosci* 9:1365–1374
- Warzecha A-K, Egelhaaf M (1999) Variability in spike trains during constant and dynamic stimulation. *Science* 283:1927–1930
- Warzecha A-K, Egelhaaf M (2001) Neuronal encoding of visual motion in real-time. In: Zanker JM, Zeil J (eds) *Processing visual motion in the real world: a survey of computational, neural, and ecological constraints*. Springer, Berlin Heidelberg New York, pp 239–277
- Warzecha A-K, Kretzberg J, Egelhaaf M (1998) Temporal precision of the encoding of motion information by visual interneurons. *Curr Biol* 8:359–368
- Warzecha A-K, Kretzberg J, Egelhaaf M (2000) Reliability of a fly motion-sensitive neuron depends on stimulus parameters. *J Neurosci* 20:8886–8896
- Warzecha A-K, Kurtz R, Egelhaaf M (2003) Synaptic transfer of dynamic motion information between identified neurons in the visual system of the blowfly. *Neuroscience* (in press)